



Subterahertz characterization of ethanol hydration layers by microfluidic system

Simon Laurette, A. Treizebre, Frederic Affouard, Bertrand Bocquet

► To cite this version:

Simon Laurette, A. Treizebre, Frederic Affouard, Bertrand Bocquet. Subterahertz characterization of ethanol hydration layers by microfluidic system. Applied Physics Letters, 2010, 97, pp.111904-1-3. 10.1063/1.3488832 . hal-00549500

HAL Id: hal-00549500

<https://hal.science/hal-00549500>

Submitted on 30 May 2022

HAL is a multi-disciplinary open access archive for the deposit and dissemination of scientific research documents, whether they are published or not. The documents may come from teaching and research institutions in France or abroad, or from public or private research centers.

L'archive ouverte pluridisciplinaire **HAL**, est destinée au dépôt et à la diffusion de documents scientifiques de niveau recherche, publiés ou non, émanant des établissements d'enseignement et de recherche français ou étrangers, des laboratoires publics ou privés.

Subterahertz characterization of ethanol hydration layers by microfluidic system

Cite as: Appl. Phys. Lett. **97**, 111904 (2010); <https://doi.org/10.1063/1.3488832>

Submitted: 23 June 2010 • Accepted: 21 August 2010 • Published Online: 13 September 2010

S. Laurette, A. Treizebre, F. Affouard, et al.



View Online



Export Citation

ARTICLES YOU MAY BE INTERESTED IN

[Silicon based microfluidic cell for terahertz frequencies](#)

Journal of Applied Physics **108**, 013102 (2010); <https://doi.org/10.1063/1.3456175>

[Invited Article: Terahertz microfluidic chips sensitivity-enhanced with a few arrays of meta-atoms](#)

APL Photonics **3**, 051603 (2018); <https://doi.org/10.1063/1.5007681>

[THz spectroscopic characterization of biomolecule/water systems by compact sensor chips](#)

Applied Physics Letters **89**, 041114 (2006); <https://doi.org/10.1063/1.2236295>

Lock-in Amplifiers
up to 600 MHz



Zurich
Instruments



Subterahertz characterization of ethanol hydration layers by microfluidic system

S. Laurette,¹ A. Treizebre,¹ F. Affouard,² and B. Bocquet^{1,a)}

¹*Institute of Electronics, Microelectronics, and Nanotechnology (IEMN), UMR CNRS 8520, University of Lille 1, 59652 Villeneuve d'Ascq, France*

²*Unité Matériaux et Transformations (UMET), UMR CNRS 8207, UFR de Physique-BAT P5, University of Lille 1, 59655 Villeneuve d'Ascq, France*

(Received 23 June 2010; accepted 21 August 2010; published online 13 September 2010)

Characterizations of ethanol hydration layers are examined through subterahertz spectroscopy of water/ethanol mixtures by using a microfluidic system. A three-component model is used to explain measurements discrepancies with the Lambert–Beer law and to determine ethanol hydration shell absorption. Moreover, the hydration shell distribution is compared with molecular dynamics simulations with a good agreement. Ethanol hydration number is then computed and it can quickly characterize only the first water hydration layer or the whole hydration shell, depending on the chosen extraction model. © 2010 American Institute of Physics. [doi:10.1063/1.3488832]

Molecules hydration-layers study is becoming an increasing field of research for biologists. Indeed, the “bound-water” at the vicinity of biomolecules such as proteins is involved in their expression, recognition, or mutual interaction.¹ Water dynamics around molecules corresponds to the terahertz (THz)-waves (100 GHz–10 THz) which are expected to be an adapted marker-free tool to determine molecules hydration-layers properties.² Indeed, several studies have shown a specific THz-absorption of “bound-water.”³ However, the huge water absorption makes THz spectroscopy of liquids complex. Powerful beams must be used⁴ or volumes must be reduced.^{5,6}

We propose to use a microsystem to probe ethanol/water solutions (Fig. 1). This original tool combines an accurate volumes-control by using microchannels and a micronic wave-confinement thanks to a THz waveguide cointegrated on a glass/silicon chip. It has already been used to follow enzymatic reactions in real-time conditions.⁷ The electromagnetic propagation is enabled by a 3- μm -width gold “Goubau line” deposited on a glass substrate.⁸ It drives the THz wave through a 50- μm -wide and 180- μm -deep microchannel dug in silicon.

Here, sub-THz measurements in the 0.05–0.11 THz band of frequencies are shown. Ethanol/water solutions with various volume ratios have been prepared and injected into the microchannels. For each mixture, complex scattering parameters (S) are measured with a vectorial network analyzer connected to the Goubau line to characterize the fluid in the microchannel. Each measurement is the result of a 30-measurement averaging for each frequency. Pure deionized water is used as a reference and is injected between each measurement, to check the measurement protocol reproducibility. A randomly chronological order of solutions has been chosen for injections to avoid any measurement bias. Raw measurements⁹ are shown in Fig. 1. Molecular dynamics (MD) simulations⁹ of liquid ethanol/water mixtures have been performed using the DL POLY program.¹⁰ The all-atom optimized potentials for liquid simulations (OPLS)

force-field¹¹ was used to model the intra and intermolecular interactions of ethanol molecules. Rigid water molecules were modeled using the TIP4P/2005 force-field.¹²

Absorption α is defined by the ratio between the transmitted power through the sample I and the incident power I_0 as $I/I_0 = A \exp(-\alpha d)$, where A is constant and d the microchannel length. $\alpha/\alpha_{\text{H}_2\text{O}}$ of each solution is extracted from (S)-parameters and is shown on Fig. 2 as a function of water concentration. These measurements are found in agreement with the ones obtained by Khurgin *et al.*¹³ and validate our device's ability to probe liquids sub-THz-dynamics. Figure 2 clearly shows that absorption decreases when ethanol concentration increases. The 95 GHz-absorption of the mixtures was also calculated from MD simulations from the Fourier transform of the total dipolar correlation function.³ It is found in fair agreement with experimental results (Fig. 2). The decrease in the mixture absorption upon increasing ethanol concentration is particularly well reproduced. It can partially be explained by the fact that ethanol absorption ($\sim 10 \text{ cm}^{-1}$) is weaker than water one ($\sim 80 \text{ cm}^{-1}$).¹⁴ Therefore, by replacing water, ethanol decreases the solution absorption. However, that should imply a linear decrease (Lambert–Beer's law).

To explain the nonlinear behavior of the absorption as a function of the water concentration, the interaction between

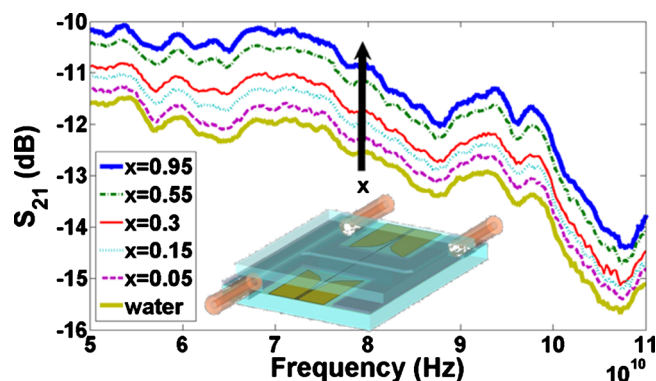


FIG. 1. (Color online) Transmission parameter S_{21} (dB) measurements as a function of $x = V_{\text{eth}}/V$ from 0.05 to 0.11 THz.

^{a)}Author to whom correspondence should be addressed. Electronic mail: bertrand.bocquet@univ-lille1.fr.

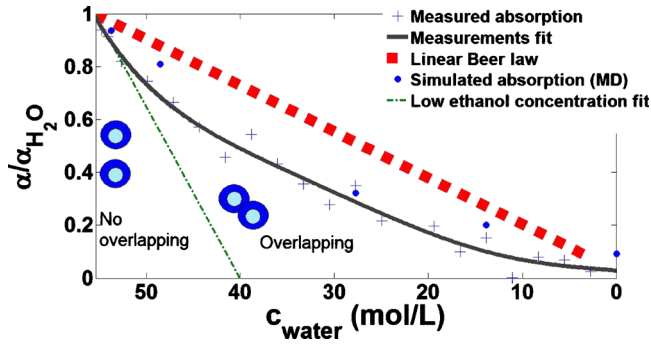


FIG. 2. (Color online) 0.95 THz normalized absorption as a function of water concentration.

ethanol and water must be considered.³ Snapshots obtained from MD simulations (Fig. 3) show that ethanol molecule may form some hydrogen bonds with water or other ethanol surrounding molecules. At the ethanol vicinity, water absorption should be reduced because of these hydrogen weak bonds. This “bound water” would form the hydration shell of ethanol molecule. At low concentration ($c_{\text{water}} > 50$ mol/l), ethanol molecules would be mainly surrounded by water molecules absorbing less than “bulk water,” which explains the linear decrease in absorption. Then, when ethanol ratio is becoming higher, hydration shells start to overlap as follows: a water molecule can be bound to several ethanol ones and therefore absorption evolution becomes non linear (Fig. 3, right).

To characterize the ethanol hydration layers, a three-component model is used.¹⁵ It decomposes the solution absorption as the sum of bulk water absorption, hydration shell absorption, and ethanol absorption as follows:

$$\alpha = \alpha_{\text{eth}} \frac{V_{\text{eth}}}{V} + \alpha_{\text{shell}} \frac{V_{\text{shell}}}{V} + \alpha_{\text{bulk}} \frac{1 - V_{\text{eth}} - V_{\text{shell}}}{V}, \quad (1)$$

α_{eth} , α_{shell} , and α_{bulk} are, respectively, the absorption coefficient of ethanol, hydration shell water, and bulk water. V_{eth}/V and V_{shell}/V are the volumic ratios of ethanol and hydration shell in the solution. α_{eth} and α_{bulk} are determined from pure ethanol and water measurements. V_{eth} and V are known. Unknown parameters are V_{shell} and α_{shell} . Here it is assumed that they are constant. Considering the low ethanol concentration area, without overlapping ($V_{\text{eth}} = kV_{\text{shell}}$), it gives the following:

$$\frac{\alpha}{\alpha_{\text{H}_2\text{O}}} = \left[\left(\frac{\alpha_{\text{eth}}}{\alpha_{\text{H}_2\text{O}}} - 1 \right) + k \left(\frac{\alpha_{\text{shell}}}{\alpha_{\text{H}_2\text{O}}} - 1 \right) \right] \frac{V_{\text{eth}}}{V} + 1. \quad (2)$$

This equation reproduces the linear evolution of absorption seen in Fig. 2 for the low ethanol concentration solutions.

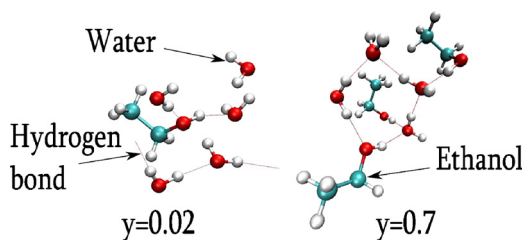


FIG. 3. (Color online) Ethanol/water configuration for $y = N_{\text{eth}}/(N_{\text{water}} + N_{\text{eth}}) = 0.02$ and 0.7 .

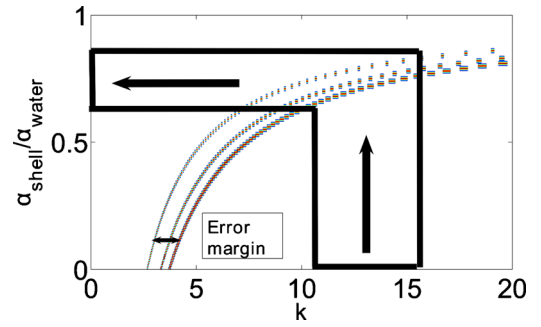


FIG. 4. (Color online) Determination of α_{shell} and k .

Solutions of this equation are given in the $(k, \alpha_{\text{shell}}/\alpha_{\text{H}_2\text{O}})$ plan (Fig. 4). To find the unique solution couple, a simple model concerning overlapping is proposed. Ethanol molecules and hydration shells are assumed to be spherical. Sphere radius of (ethanol+hydration shell) is called a . Assuming that just before overlapping, N_{over} ethanol molecules are homogeneously distributed in a volume V (Fig. 5), it comes as follows:

$$N_{\text{over}} \times (2a)^3 = V, \quad (3)$$

N_{over}/V can be determined with Fig. 2, when absorption deviates from low-ethanol-concentration linear evolution. This deviation is evaluated by observing the relative error δ between the low-concentration fit and the whole-concentration fit as follows: we assume that the overlap condition is filled for δ between 5% and 10%. With this condition, $c_{\text{water}} = 51 \pm 0.8$ mol/l. Thus, a has been found equal to 5.4 ± 0.4 Å. Considering the 4.46 Å ethanol molecule diameter,¹⁶ it implies that the hydration shell length is about 3.2 ± 0.4 Å. k can now be calculated in the spherical approximation; $k = 13 \pm 2.5$. It is reported in Fig. 4 and then, $\alpha_{\text{shell}}/\alpha_{\text{H}_2\text{O}} = 0.72 \pm 0.1 < 1$, which confirms that bound water absorption is lower than bulk water one. k and $\alpha_{\text{shell}}/\alpha_{\text{H}_2\text{O}}$ are reported in Eq. (2) and the absorption computed by the three-component-model accurately fits the linear low-ethanol-concentration evolution. To valid this method, comparison with MD results has been done. In Fig. 6, ethanol/water pair distribution function $g(r)$ normalized by bulk water distribution around an ethanol molecule is presented. It shows that the hydration shell seems to be inhomogeneous and constituted of two hydration layers and gives $a \sim 5.5$ Å, which well corresponds to the experimental value.

The hydration number N_h is the number of water molecules in the ethanol hydration shell. It was determined from MD simulations by integrating $g(r)$ between 0 and 3.3 Å (first hydration layer) and 0 and 5.5 Å (whole hydration shell), respectively, corresponding to the first and second

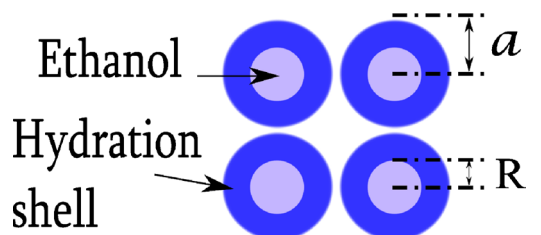


FIG. 5. (Color online) Model for configuration just before overlapping.

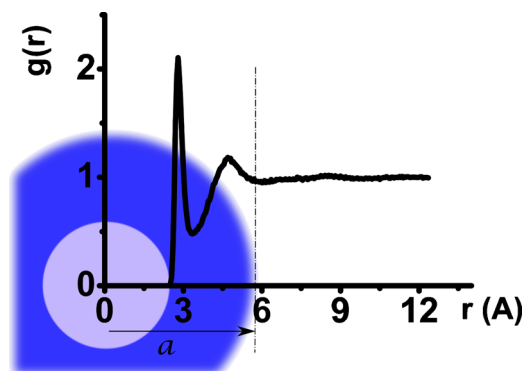


FIG. 6. (Color online) Water distribution around ethanol molecule.

$g(r)$ minima. A value of $N_h=2.7$ was obtained for the first hydration layer and $N_h \sim 26$ for whole hydration shell. Experimentally, assuming that $V_{\text{shell}}=4(a^3-R^3)\pi/3$ and that the hydration shell density ρ is the same as bulk water, it comes $N_h=\rho N_A V_{\text{shell}}/M_{\text{H}_2\text{O}}$ where N_A is the Avogadro number. This leads to $N_h \sim 30$ which is closed to simulation results when the first and the second hydration layers are considered. The difference may be explained by the constant density assumption, which disagrees with Fig. 6. Khurgin's result¹³ was $N_h=4$, assuming that hydration shell absorption coefficient was equal to zero. This latter hydration number is closer to the value obtained from MD simulations by integrating the first peak of $g(r)$. Consequently, depending on the model taken for hydration shell characterization, one could probe the entire hydration shell or only the first layer of water molecules around ethanol.

The use of a Monte Carlo algorithm⁴ to fit the three-component-model not only in the low ethanol concentration linear region but in the whole panel of concentrations would be useful. Besides, we show that bound water absorption is lower than bulk water one, because of hydrogen bonds which decrease water mobility at the ethanol vicinity. However, in sugar hydration studies, from 1 to 3 THz, hydration shell absorbs more than bulk water as follows:^{15,17} presence of hydrogen bonds is evoked and the magnified absorption is due to their excitation. Increasing frequencies in our mea-

surements is planned to confirm this behavior. The present investigation thus motivates additional works in order to be fully validated.

To conclude, thanks to water absorption, one can probe indirectly molecules in solution through their influence on water state. It is the molecule "mold of water" which is probed and which might be the molecule signature. Consequently, the huge absorption of water, which led to use powerful beams or to reduce sample volumes, has been transformed in a useful way to detect molecules. Next works will be done with more complex molecules like proteins with this microsystem as an experimental tool to get sensitive and reproducible measurements.

¹P. W. Fenimore, H. Frauenfelder, B. H. McMahon, and R. D. Young, *Proc. Natl. Acad. Sci. U.S.A.* **101**, 14408 (2004).

²S. K. Pal, J. Peon, and A. H. Zewail, *Proc. Natl. Acad. Sci. U.S.A.* **99**, 1763 (2002).

³D. M. Leitner, M. Gruebele, and M. Havenith, *HFSP J.* **2**, 314 (2008).

⁴S. Ebbinghaus, S. J. Kim, M. Heyden, U. Heugen, M. Gruebele, D. M. Leitner, and M. Havenith, *Proc. Natl. Acad. Sci. U.S.A.* **104**, 20749 (2007).

⁵J. Xu, K. W. Plaxco, and S. J. Allen, *Protein Sci.* **15**, 1175 (2006).

⁶T. Ohkubo, M. Onuma, J. Kitagawa, and Y. Kadoya, *Appl. Phys. Lett.* **88**, 212511 (2006).

⁷A. Abbas, A. Treizebre, P. Supiot, N. E. Bourzgui, D. Guillochon, D. Vercaigne-Marko, and B. Bocquet, *Biosens. Bioelectron.* **25**, 154 (2009).

⁸A. Treizebre and B. Bocquet, *Int. J. Nanotechnol.* **5**, 784 (2008).

⁹A. Lerbret, P. Bordat, F. Affouard, M. Descamps, and F. Migliardo, *J. Phys. Chem. B* **109**, 11046 (2005).

¹⁰W. Smith, The DL POLY Molecular Simulation Package, CSE Department, STFC Daresbury Laboratory.

¹¹W. L. Jorgensen, D. Maxwell, and J. Tirado-Rives, *J. Am. Chem. Soc.* **118**, 11225 (1996).

¹²J. L. F. Abascal and C. Vega, *J. Chem. Phys.* **123**, 234505 (2005).

¹³Y. I. Khurgin, V. A. Kudryashova, and V. A. Zavizion, *J. Commun. Technol. Electron.* **41**, 640 (1996).

¹⁴T. Sato and R. Buchner, *J. Phys. Chem. A* **108**, 5007 (2004).

¹⁵U. Heugen, G. Schwaab, E. Bründermann, M. Heyden, X. Yu, D. M. Leitner, and M. Havenith, *Proc. Natl. Acad. Sci. U.S.A.* **103**, 12301 (2006).

¹⁶E. Ivanova, D. Damgaliev, and M. Kostova, *J. Univ. Chem. Technol. Metallurgy* **44**, 267 (2009).

¹⁷M. Heyden, E. Bründermann, U. Heugen, G. Niehues, D. M. Leitner, and M. Havenith, *J. Am. Chem. Soc.* **130**, 5773 (2008).